

TWO-DIODE MODELLING OF PEROVSKITE SOLAR CELLS AND PARAMETER EXTRACTION USING THE LAMBERT W FUNCTION

Ana Bărar¹, Cristian Boscornea², Maria Bălășoiu^{3,4}, Doina Mănănilă-Maximean⁵

This paper provides a Lambert W-based explicit form for the total current equation of a double-diode equivalent circuit used to model solar cell devices. A sample perovskite solar cell was fabricated, and the calculated expression was used on the experimental data of the sample cell, in order to extract its device parameters. The results were compared with the values obtained using the explicit form of the single-diode equivalent model, in order to verify accuracy. Moreover, a further study of the explicit Lambert W-based expression for the double-diode model was conducted, by varying the value of current coefficients, thus determining their optimal values for accurate data fitting.

Keywords: photovoltaic cell, perovskite solar cell, double-diode model, W Lambert function

1. Introduction

Photovoltaic technology has witnessed a rapid progress in the past decades, due to the development of novel device performance enhancement methods, such as doping techniques [1–7], solar concentrators built from metasurface structures [8–10], or the discovery of novel composite or hybrid materials [11–13], with light absorbing properties. Among these materials, perovskite-based solar cells (PSC), in particular, have been reported to yield outstanding power conversion efficiencies [14, 15]. This promising performance is due to the structure of the perovskite active layer, which exhibits remarkable optical absorption properties, as well as long charge carrier diffusion length and direct bandgap transition [16]. However, several crucial drawbacks [17–19] must still be overcome in PSC technology and fabrication, before they may be considered as a viable alternative to silicon solar cells, the main solar energy converters marketed today. Most of these deficiencies are of a structural nature, such as rapid degradation, poor film quality and thickness, sensitivity to heat and humidity, and high toxicity due to the presence of lead (*Pb*) compounds. Accurate device and material characterizations are crucial for resolving these shortcomings.

The two most widely used models in solar cell device characterization are the single-diode equivalent model (see figure 1a), and its more complex derivation, the double-diode model (see figure 1b).

¹Lecturer, Department of Electronic Technology and Reliability, University POLITEHNICA of Bucharest, Romania, e-mail: ana.barar@upb.ro

²Associate Professor, Department of Bioresources and Polymer Science, University POLITEHNICA of Bucharest, Romania

³Joint Institute for Nuclear Research, Dubna, Russia

⁴Horia Hulubei Institute of Physics and Nuclear Engineering, Bucharest,

⁵Professor, Physics Department, University POLITEHNICA of Bucharest, Romania

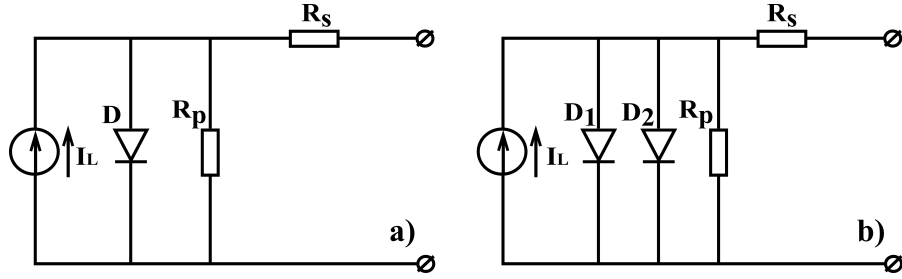


FIGURE 1. Equivalent circuit models used for solar cell device characterization: a) the one diode model, and b) the two-diode model, where I_L is the current source which models the photocurrent generated within the cell under illumination, diodes D and D_1 model the p-n junction in the cell, diode D_2 represents the charge carriers recombination that takes place in the junction at low voltages, the series resistance R_s models the interface defects found between the active layer and the electrodes, and the parallel (or shunt) resistance R_p models the bulk defects in the active layer of the cell.

The single-diode model was extensively studied [20–23]. The total current I equation derived from this model is transcendental:

$$I = I_L - I_0 \left[\exp \left(\frac{e(U + R_s I)}{\gamma k T} \right) - 1 \right] - \frac{U + R_s I}{R_p} \quad (1)$$

where e is the elementary electron charge, U is the voltage yielded by the cell, k is the Boltzmann constant, T is the temperature, I_0 is the dark saturation current of diode D , γ is the ideality factor of diode D , respectively. An explicit form for equation (1) was calculated with the use of the Lambert W function:

$$I = \frac{W \left[\frac{e}{\gamma k T} \frac{R_s R_p I_0}{(R_s + R_p)} \exp \left[\frac{e}{\gamma k T} \frac{R_p (U + R_s I_0 + R_s I_L)}{(R_s + R_p)} \right] \right]}{\frac{e}{\gamma k T} R_s} - \frac{R_p}{(R_s + R_p)} \left(I_0 + I_L - \frac{U}{R_p} \right) \quad (2)$$

This paper discusses the double-diode model, which provides a more accurate approximation of device parameters. Each component in the double-diode equivalent circuit models a certain effect that appears in the solar cell under illumination, as follows: the current source I_L models the photocurrent generated within the cell under illumination, diode D_1 models the p-n junction in the cell, diode D_2 represents the charge carriers recombination that takes place at the p-n junction at low voltages, the series resistance R_s models the interface defects found between the active layer and the electrodes, and the parallel (or shunt) resistance R_p models the bulk defects in the active layer of the cell. The total current I yielded by this circuit represents the current produced by the cell under illumination, and it is described by the following equation:

$$I = I_L - I_{01} \left[\exp \left(\frac{e(U + R_s I)}{\gamma_1 k T} \right) - 1 \right] - I_{02} \left[\exp \left(\frac{e(U + R_s I)}{\gamma_2 k T} \right) - 1 \right] - \frac{U + R_s I}{R_p} \quad (3)$$

where I_{01} is the dark saturation current of diode D_1 , γ_1 is the ideality factor of diode D_1 , I_{02} is the dark saturation current of diode D_2 , γ_2 is the ideality factor of diode D_2 , respectively. The seven circuit parameters necessary for solar cell characterization are: I_L , R_s , R_p , γ_1 , γ_2 , I_{01} , I_{02} , and they must be extracted from equation (3). However, equation (3) is transcendental (or implicit), therefore it cannot be resolved analytically, numerical methods must be considered for parameter extraction. Based on previous work conducted and published over the single-diode model [20, 21], this paper proposes a method involving the Lambert W function, tailored for extracting the parameters of interest. The method is applied on the experimental data obtained for a fabricated sample perovskite solar cell, and the results are compared with the values obtained using the explicit Lambert W-based expression deduced from the single-diode model, in order to verify accuracy. Furthermore, a study of the influence of the current coefficient over the behavior of the double-diode is conducted, and the results indicate its optimal value for accurate data fitting.

2. Lambert W function for the double-diode model

The Lambert W function is mathematically defined as [24]:

$$z = W(z) \exp(W(z)) \quad (4)$$

where $z \in C$. Among its many applications, this function is also used for solving transcendental equations or algorithm analysis [23–25]. The Lambert W function is used here in order to obtain an analytic dependency between the voltage U and the total current I , from equation (3). To do this, equation (3) must be rearranged in the following form [24]:

$$X = Y \exp(Y) \leftrightarrow Y = W(X) \quad (5)$$

where Y is a function that depends on I . However, equation (3) contains a sum of two exponential expressions, which poses considerable difficulties in achieving this task. In order to overcome these impediments, the following approximations were considered:

- (1) The dark saturation currents of diodes D_1 and D_2 are considered identical, $I_{01} = I_{02} = I_0$;
- (2) The ideality factors of diodes D_1 and D_2 are equal to 1 and 2, respectively ($\gamma_1 = 1$, $\gamma_2 = 2$). Therefore, equation (3) becomes:

$$I = I_L - I_0 \left[\exp \left(\frac{e(U + R_s I)}{kT} \right) - 1 \right] - I_0 \left[\exp \left(\frac{e(U + R_s I)}{2kT} \right) - 1 \right] - \frac{U + R_s I}{R_p} \quad (6)$$

Following the approach similar to the one presented in [26], equation (6) is then split into a sum of two currents I_1 and I_2 , each containing only one exponential expression, as follows:

$$I = I_1 + I_2 \quad (7)$$

where I_1 is:

$$I_1 = nI_L - I_0 \left[\exp \left(\frac{e(U + R_s I)}{kT} \right) - 1 \right] - n \frac{U + R_s I}{R_p} \quad (8)$$

and I_2 is:

$$I_2 = (1-n)I_L - I_0 \left[\exp \left(\frac{e(U+R_s I)}{2kT} \right) - 1 \right] - (1-n) \frac{U+R_s I}{R_p} \quad (9)$$

In equations (8) and (9), n is a coefficient denoting the separate contribution of I_1 and I_2 to the total current I , and is confined to the interval $n \in (0; 1)$. The Lambert W functions are calculated for equations (8) and (9) separately, yielding the following explicit expressions for currents I_1 and I_2 :

$$I_1 = \left[\frac{nR_p I_L - nU + R_p I_0}{n(R_s + R_p)} \right] - \frac{kT}{eR_s} W \left[\frac{eR_s R_p I_0}{kT n(R_s + R_p)} \exp \left[\frac{eU}{kT} + \frac{eR_s}{kT} \left(\frac{nR_p I_L - nU + R_p I_0}{n(R_s + R_p)} \right) \right] \right] \quad (10)$$

$$I_2 = \left[\frac{(1-n)R_p I_L - (1-n)U + R_p I_0}{(1-n)(R_s + R_p)} \right] - \frac{2kT}{eR_s} W \left[\frac{eR_s R_p I_0}{2kT(1-n)(R_s + R_p)} \exp \left[\frac{eU}{2kT} + \frac{eR_s}{2kT} \left(\frac{(1-n)R_p I_L - (1-n)U + R_p I_0}{(1-n)(R_s + R_p)} \right) \right] \right] \quad (11)$$

The Lambert W function for the total current I , defined by equation (3), may be obtained by adding expressions (10) and (11) together:

$$I = \left[\frac{nR_p I_L - nU + R_p I_0}{n(R_s + R_p)} \right] - \frac{kT}{eR_s} W \left[\frac{eR_s R_p I_0}{kT n(R_s + R_p)} \exp \left[\frac{eU}{kT} + \frac{eR_s}{kT} \left(\frac{nR_p I_L - nU + R_p I_0}{n(R_s + R_p)} \right) \right] \right] + \left[\frac{(1-n)R_p I_L - (1-n)U + R_p I_0}{(1-n)(R_s + R_p)} \right] - \frac{2kT}{eR_s} W \left[\frac{eR_s R_p I_0}{2kT(1-n)(R_s + R_p)} \exp \left[\frac{eU}{2kT} + \frac{eR_s}{2kT} \left(\frac{(1-n)R_p I_L - (1-n)U + R_p I_0}{(1-n)(R_s + R_p)} \right) \right] \right] \quad (12)$$

The following device parameters are extracted using expression (12): short-circuit current I_{sc} , open-circuit voltage U_{oc} , dark saturation current I_0 , series resistance R_s , parallel resistance R_p , maximum power point P_m , fill-factor FF , and power-conversion efficiency η .

3. Perovskite solar cell modelling and device characterization using the double-diode model: fabrication procedure and numerical processing

3.1. Fabrication process

The experimental data used for testing the Lambert W function deduced in the section above belong to a $CH_3NH_2PbI_3$ perovskite solar cell, that was fabricated by following the procedure below:

- (1) Heating of Carbon electrodes, deposited on conducting glass at $430^\circ C$, for 30 minutes;
- (2) Application of 0.01 ml precursor solution over the carbon layer;

(3) Heating of the carbon layer with added precursor solution at 50°C, for 15 minutes. The precursor solution reacts with the Carbon layer, thus forming the perovskite active layer of the cell ($CH_3NH_2PbI_3$);

(4) Application of the adhesive gasket and the protective glass;

(5) Heating of the resulted cell at 110°C, in order to ensure the melting of the adhesive gasket and the sealing of the cell.

The precursor solution is a mixture of lead iodide (PbI), methyl ammonium iodide, 5-aminovaleric acid hydroiodide, and gamma-butyrolactone (solvent), designed to react with the Carbon layer, in order to form the perovskite layer ($CH_3NH_2PbI_3$).

3.2. Results and discussions

Values for parameters I_0 , R_s , and R_p were extracted by fitting equations (2) and (12) to the experimental data of the sample cell, using the least squares method. The initial values used in these calculations, were extracted from the experimental curve with the asymptotic approximation method. Figures 2 and 3 show fitted current-voltage (I-V) and power-voltage (P-V) curves which were traced by using the sets of parameters I_0 , R_s , and R_p , obtained with the asymptotic approximation, the single-diode model, and the double-diode model, respectively. The values of these parameters are shown in table 1, along with the values of parameters (I_{sc} , U_{oc} , P_m , FF , η), extracted from each fitted curve, and the experimental curve, respectively.

TABLE 1. Values extracted for the sample perovskite solar cell device parameters, using three different methods of extraction, where 1D LW – one-diode model Lambert W function, 2D LW – double-diode model Lambert W function.

Extraction method	I_{sc} (mA)	U_{oc} (V)	I_0 (pA)	R_s (Ω)	R_p ($k\Omega$)	P_m (mW)	FF	η (%)
Experimental data	0.4500	0.700	-	-	-	0.1936	0.6146	0.5378
Asymptotic approximation	0.4500	0.700	10^{-2}	150	10	0.20945	0.6649	0.5818
1D LW	0.4500	0.700	$3 \cdot 10^{-2}$	200	50	0.19672	0.6245	0.5465
2D LW	0.4500	0.700	$2 \cdot 10^{-3}$	200	100	0.1931	0.6131	0.5364

The double-diode model yielded a dark saturation current $I_0 = 2 \cdot 10^{-3}$ pA, a series resistance $R_s = 200\Omega$, and a parallel resistance $R_p = 100k\Omega$, and the I-V curve that was fitted using these values yielded a maximum power point $P_m = 0.1931mW$, a fill-factor $FF = 0.6131$, and a power-conversion efficiency $\eta = 0.5364\%$. As shown in table 1, these parameters are much closer in value to the experimental data, than are the results obtained with the single-diode model, which indicates the double-diode model's superior accuracy.

For a more in-depth understanding of the double-diode model, a study was conducted regarding the influence of the current coefficient n over the overall behavior of the model. By maintaining the values of I_0 , R_s , and R_p constant in equation (12), several I-V and P-V curves were traced, for different values of $n \in (0; 1)$, as shown in figures 4 and 5. The parameters extracted from the I-V curves shown in figure 4 are presented in table 2. By comparing the values shown in table 2 to the experimental values, one may conclude that the optimal value for the current coefficient n is $n = 0.5$.

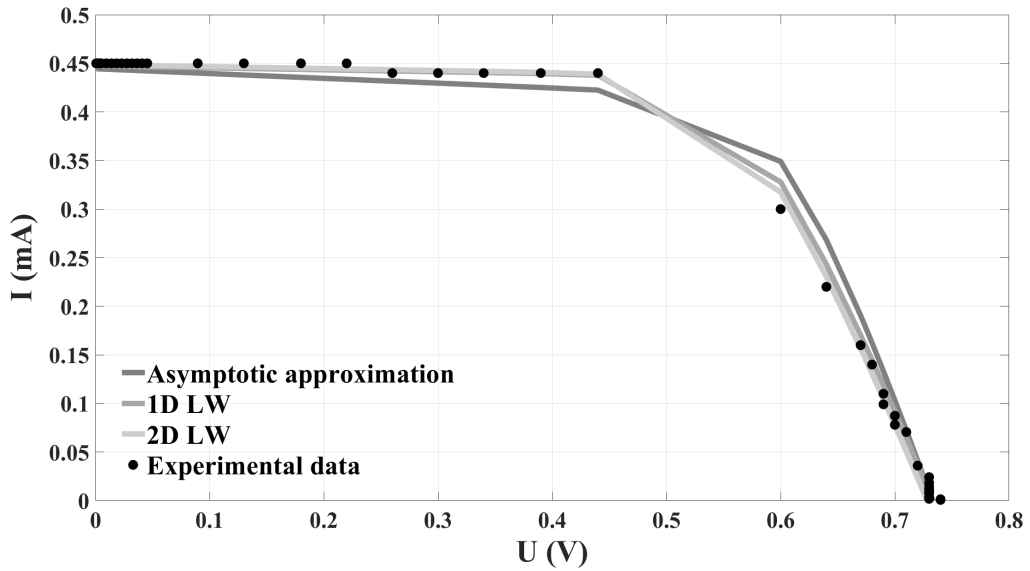


FIGURE 2. Fitted current-voltage (I-V) curves traced using the parameters extracted with the rough approximation method, the single-diode Lambert W function (1D LW), and the double-diode Lambert W function (2D LW), respectively

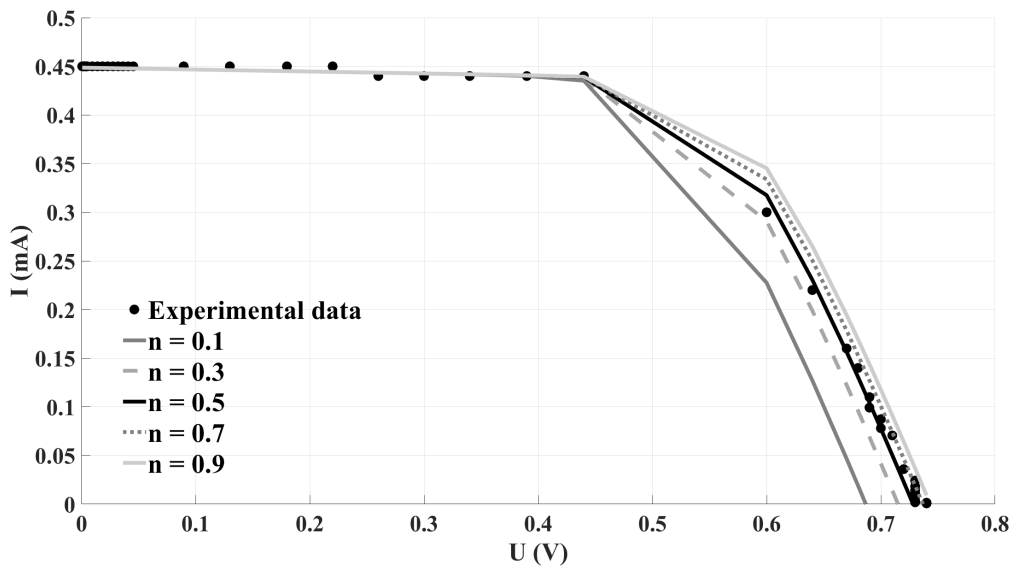


FIGURE 4. Fitted current-voltage (I-V) curves traced using the parameters extracted with the double-diode Lambert W function (2D LW), for different values of the current coefficient n

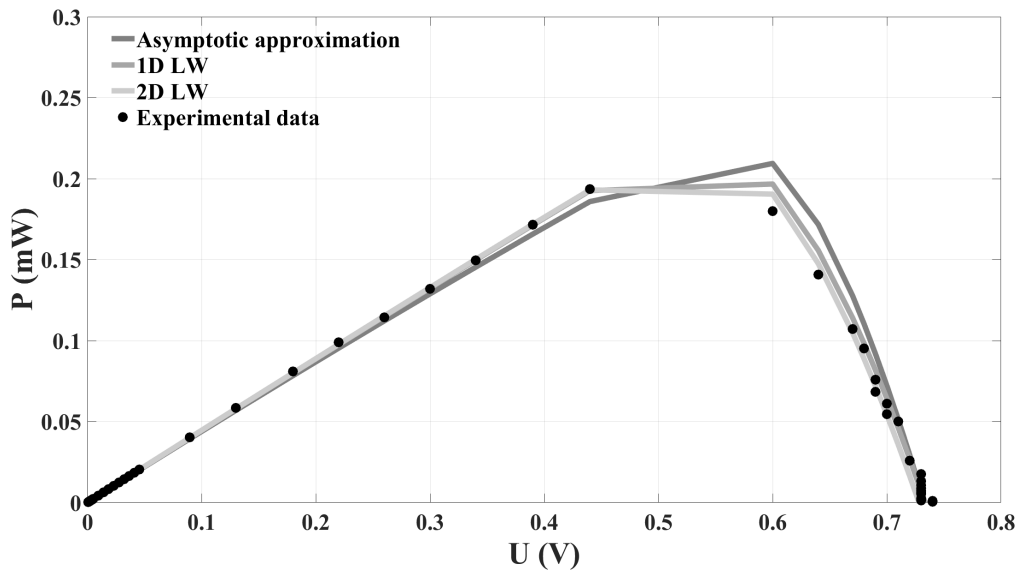


FIGURE 3. Fitted power-voltage (P-V) curves traced using the parameters extracted with the rough approximation method, the single-diode Lambert W function (1D LW), and the double-diode Lambert W function (2D LW), respectively

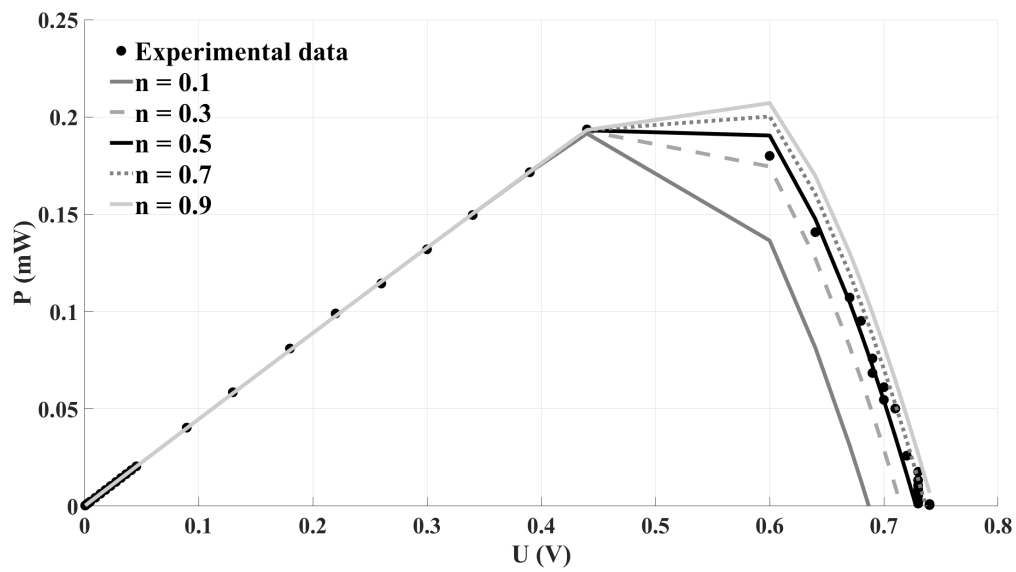


FIGURE 5. Fitted power-voltage (P-V) curves traced using the parameters extracted with the double-diode Lambert W function (2D LW), for different values of the current coefficient n

TABLE 2. Parameters extracted from the I-V curves traced with the double-diode model Lambert W function, for different values of current coefficient n

Value of n	P_m (mW)	FF	η (%)
0.1	0.1915	0.6079	0.5319
0.3	0.1928	0.6122	0.5357
0.5	0.1931	0.6131	0.5346
0.7	0.2003	0.6358	0.5563
0.9	0.2071	0.6576	0.5754
Experimental values	0.1936	0.6146	0.5378

4. Conclusions

This paper demonstrates a Lambert W function-based explicit equation for the total current I of the double-diode equivalent circuit used to model solar cell devices. The explicit form of the total current I was deduced from the total current transcendental form, by splitting the equation into a sum of two currents, I_1 and I_2 , each containing one exponential component, followed by the calculation of the Lambert W function for both I_1 and I_2 . The explicit form of I was then obtained by adding the two explicit expressions of I_1 and I_2 . This expression, along with the explicit expression for the single-diode model, were tested on the experimental data of a fabricated sample perovskite solar cell. By comparing the results obtained with the double-diode model, against the values obtained with the single-diode model, the superior accuracy of the double-diode model is demonstrated.

Furthermore, the influence of the current coefficient n over the overall behavior of the double-diode model was studied by tracing several current-voltage (I-V) and power-voltage (P-V) curves based on the explicit Lambert W expression of the model, for different values of n . The values of the maximum power point P_m , the fill-factor FF , and the power-conversion efficiency η , were extracted from each curve, and by comparing the results to the experimental data, it was concluded that a current coefficient of value $n = 0.5$ is optimal for accurate data fitting with the Lambert W-based explicit equation demonstrated in this paper for the double-diode model.

Acknowledgements

The authors acknowledge the support of Project RO-JINR, position 64 in IUCN Order no.365/11.05.2021, Theme 04-4-1141-2020/2022.

REFERENCES

- [1] Zhang, Z. and Gao, Q. and Guo, J. and Zhang, Y. and Han, Y. and Ao, J. and Jeng, M.-J. and Liu, F. and Liu, W. and Zhang, Y., Over 10% efficient pure cztse solar cell fabricated by electrodeposition with ge doping, *Solar RRL* **4**(5), 2000059 (2020).
- [2] Liu, B. and Guo, J. and Hao, R. and Wang, L. and Gu, K. and Sun, S. and Aierken, A., Effect of na doping on the performance and the band alignment of czts/cds thin film solar cell, *Solar Energy* **201**, 219–226 (2020).
- [3] Barar, A. and Manaila-Maximean, D., Ruthenium-based dssc efficiency optimization by graphene quantum dot doping, *UNIVERSITY POLITEHNICA OF BUCHAREST SCIENTIFIC BULLETIN-SERIES A-APPLIED MATHEMATICS AND PHYSICS* **83**(2), 309–316 (2021).
- [4] Cirtoaje, C. and Petrescu, E. and Stan, C. and Rogachev, A., Electric freedericksz transition in nematic liquid crystals with graphene quantum dot mixture, *Applied Surface Science* **487**, 1301–1306 (2019).

[5] Petrescu, E. and Cirtoaje, C. and Danila, O., Dynamic behavior of nematic liquid crystal mixtures with quantum dots in electric fields, *Beilstein journal of nanotechnology* **9**(1), 399–406 (2018).

[6] Petrescu, E. and Cirtoaje, C., Dynamic behavior of a nematic liquid crystal with added carbon nanotubes in an electric field, *Beilstein journal of nanotechnology* **9**(1), 233–241 (2018).

[7] Cirtoaje, C. and Petrescu, E., The influence of graphene nanoplatelets on the freedericksz transition threshold in nematic liquid crystals, in *Advanced Topics in Optoelectronics, Microelectronics, and Nanotechnologies IX*, **10977**, 109770J, International Society for Optics and Photonics (2018).

[8] Dănilă, O. and Mănilă-Maximean, D. and Bărar, A. and Loiko, V. A., Non-layered gold-silicon and all-silicon frequency-selective metasurfaces for potential mid-infrared sensing applications, *Sensors* **21**(16) (2021).

[9] Danila, O. and Manaila-Maximean, D., Bifunctional metamaterials using spatial phase gradient architectures: Generalized reflection and refraction considerations, *Materials* **14**(9) (2021).

[10] Danila, O., Polyvinylidene fluoride-based metasurface for high-quality active switching and spectrum shaping in the terahertz g-band, *Polymers* **13**(11) (2021).

[11] Eom, T. and Kim, S. and Agbenyeku, R. E. and Jung, H. and Shin, S. M. and Lee, Y. K. and Kim, C. G. and Chung, T.-M. and Jeon, N. J. and Park, H. H. and others, Copper oxide buffer layers by pulsed-chemical vapor deposition for semitransparent perovskite solar cells, *Advanced Materials Interfaces* **8**(1), 2001482 (2021).

[12] Wang, Y. and Lan, Y. and Song, Q. and Vogelbacher, F. and Xu, T. and Zhan, Y. and Li, M. and Sha, W. E. and Song, Y., Colorful efficient moiré-perovskite solar cells, *Advanced Materials* **33**(15), 2008091 (2021).

[13] Ye, F. and Ma, J. and Chen, C. and Wang, H. and Xu, Y. and Zhang, S. and Wang, T. and Tao, C. and Fang, G., Roles of maci in sequentially deposited bromine-free perovskite absorbers for efficient solar cells, *Advanced Materials* **33**(3), 2007126 (2021).

[14] Jeong, J. and Kim, M. and Seo, J. and Lu, H. and Ahlawat, P. and M., Aditya and Yang, Y. and Hope, M. A. and Eickemeyer, F. T. and Kim, M. and others, Pseudo-halide anion engineering for α -fapbi 3 perovskite solar cells, *Nature* **592**(7854), 381–385 (2021).

[15] Yoo, J. J. and Seo, G. and Chua, M. R. and Park, T. G. and Lu, Y. and Rotermund, F. and Kim, Y.-K. and Moon, C. S. and Jeon, N. J. and Correa-Baena, J.-P. and Bulović, V. and Shin, Seong S. and Bawendi, M. G. and Seo, J., Efficient perovskite solar cells via improved carrier management, *Nature* **590**(7847), 587–593 (2021).

[16] G. Kim and H. Min and K.S. Lee and D. Y. Lee and S. M. Yoon and S. I. Seok, Impact of strain relaxation on performance of alphax3b1;formamidinium lead iodide perovskite solar cells, *Science* **370**(6512), 108–112 (2020).

[17] U. Krishnan and M. Kaur and M. Kumar and A. Kumar, Factors affecting the stability of perovskite solar cells: a comprehensive review, *Journal of Photonics for Energy* **9**(2), 1 – 42 (2019).

[18] Leguy, A. M. A. and Hu, Y. and Campoy-Quiles, M. and Alonso, M. I. and Weber, O. J. and Azarhoosh, P. and Van Schilfgaarde, M. and Weller, M. T. and Bein, T. and Nelson, J. and others, Reversible hydration of ch3nh3pbi3 in films, single crystals, and solar cells, *Chemistry of Materials* **27**(9), 3397–3407 (2015).

[19] Goyer, Robert A, Lead toxicity: current concerns., *Environmental health perspectives* **100**, 177–187 (1993).

[20] Bărar, A. and Mănilă-Maximean, D. and Dănilă, O. and Vlădescu, M., Parameter extraction of an organic solar cell using asymptotic estimation and lambert w function, in *Advanced Topics in Optoelectronics, Microelectronics, and Nanotechnologies VIII*, **10010**, 1001034, International Society for Optics and Photonics (2016).

[21] Bărar, A. and Vlădescu, M. and Ţchiopu, P., Theoretical characterization and physical parameter determination for polymer-blend bulk heterojunction organic solar cells, *UPB Scientific Bulletin Series A* **80**(3), 217–226 (2018).

[22] del Pozo, G. and Romero, B. and Arrendondo, B., Extraction of circuital parameters of organic solar cells using the exact solution based on lambert w-function, *Proceedings of SPIE* **8435** (2012).

[23] Jain, A. and Kapoor, A., A new approach to study organic solar cell using lambert w-function, *Solar Energy Materials and Solar Cells* **86**, 197–205 (2005).

[24] R. M. Corless and G. H. Gonnet and D. E. G. Hare and D. J. Jeffrey and D. E. Knuth, On the lambert w function, *ADVANCES IN COMPUTATIONAL MATHEMATICS* **5**, 329–359 (1996).

[25] Mitroi, M. R. and Ninulescu, V. and Fara, L., Performance optimization of solar cells based on heterojunctions with cu 2 o: numerical analysis, *Journal of Energy Engineering* **143**(4), 04017005 (2017).

[26] *Gao, X. and Cui, Y. and Hu, J. and Xu, G. and Yu, Y.*, Lambert w-function based exact representation for double diode model of solar cells: Comparison on fitness and parameter extraction, *Energy conversion and management* **127**, 443–460 (2016).